

ON FUNDAMENTALS AND APPLICATIONS OF SUPERHYDROPHOBICITY IN PAPERMAKING AND PACKAGING

Agne Swerin and Martin Wåhlander

YKI, Institute for Surface Chemistry, Box 5607, SE-114 86
Stockholm, Sweden

Corresponding author: agne.swerin@yki.se

Fundamental material science investigations of superhydrophobicity in recent years has evolved toward industrial applications and recently to papermaking and packaging. The present study concerns both fundamental and applied aspects of superhydrophobicity. An industrially viable process for a one-step waterborne superhydrophobic coating was developed. It is shown that different measures of the degree of superhydrophobicity are needed depending on the final application whether this may be self-cleaning or stain repellent action. Fundamental aspects of superhydrophobicity were investigated using silica wafers roughened by a particulate formulation containing nanosize silica particles, which were fixed to the substrate by calcination. After hydrophobization by silylation, the forces between a colloidal superhydrophobized silica probe, made according to a similar procedure, and these surfaces were measured by Atomic Force Colloidal Probe Microscopy. The results show an extremely long-range interaction force and a large influence of surfactant and surfactant concentration. The results would prove useful in designing robust superhydrophobic application in the papermaking and packaging industry and also imply that coating and printing technique could be used for controlled deposition of superhydrophobized layers or areas.

INTRODUCTION

Recent reports [1–4] have shown that superhydrophobic (SH) surfaces [5] can be achieved for paper and packaging substrates relevant to industrial applications. The area has received a lot of attraction due to the possibility to mimic, for example, the self-cleaning behaviour, so called lotus leaf effect. The specific requirements to achieve an ultrahydrophobic or SH substrate surface is governed by a combination of controlled surface roughness and controlled hydrophobicity. This can be achieved in two separate process steps or, more preferably for industrial applications, in one combined step. The applications in mind could be e.g. water repellent surfaces, protection against condensation of ice and water vapour, stain repellency through self-cleaning, microfluidic control of drop motions, entertainment, antifouling or antireflex treatment. For successful papermaking applications several process and product demands have still to be met, such as mechanical properties, adhesion and friction, optical properties, taste and odor, and the treatment should be applied in a viable process not requiring radically new process equipment. The basic requirements for superhydrophobicity is given by the Young equation and the surface roughness impact by the Wenzel and Cassie-Baxter relationships, as summarized by Feng *et al.* [6], i.e. wetted contact between the liquid and the rough substrate (Wenzel's mode) or non-wetted contact between the liquid and the rough substrate (Cassie's mode) or the combination an intermediate state between the Wenzel and the Cassie modes. The present study discusses both fundamental and applied aspects of SH coatings.

The contact angle of a water droplet depends on the chemistry of the surface. If the surface is polar, the water atoms are attracted by the charges due to its dipolar nature. The droplet spreads out on the surface. However, if the surface is nonpolar and lacks charges, the water droplet does not like to be in contact with the surface and therefore forms as small contact area as possible, which give rise to a large contact angle (CA), see Figure 1.

When the CA is $\geq 90^\circ$ the surface is defined as hydrophobic. The maximum water CA attained on a flat surface is about 130° . This was achieved by stretching a flexible substrate during the self-assembly of an organosilane monolayer. The strain was then released in order to increase the close-packing of organosilane and decrease the structural defects [7]. Surfaces are defined as superhydrophobic when the CA exceeds 150° . However, surface chemistry by itself is not sufficient to achieve such high CAs and requires a certain surface roughness, as discusse below.

Young's equation describes the CA of a droplet on a flat solid surface, θ_0 :

$$\cos \theta_0 = \frac{\gamma_{SV} - \gamma_{SL}}{\gamma_{LV}} \quad (1)$$

where γ_{ij} is the surface tension of the solid-vapour, solid-liquid and liquid-vapour interfaces, respectively. This expression only determines the interfacial tensions from surface chemistry.

The Wenzel model [8] describes a complete wetting behaviour of a rough surface beneath a water droplet as shown in Figure 2b. The water droplet imbibes into the surface cavities and remains pinned to the surface, which magnifies the wetting property of the surface and leads to a high hysteresis or a high threshold sliding angle. The relationship between the CA of a liquid on a flat surface θ_0 and the CA of the same liquid on a rough surface θ_w can be written as:

$$\cos \theta_w = R_f \cos \theta_0 \quad (2)$$

where the surface roughness (R_f) is defined as the ratio of the solid-liquid contact area (A_{actual} , the actual surface area) to its projection on a flat plane (A_F , the apparent surface area):

$$R_f = \frac{A_{actual}}{A_F} \quad (3)$$

An increase of R_f increases the area of the solid, which geometrically modifies hydrophobicity at a moderate level. A thorough discussion has been made extending this to different geometries [9].

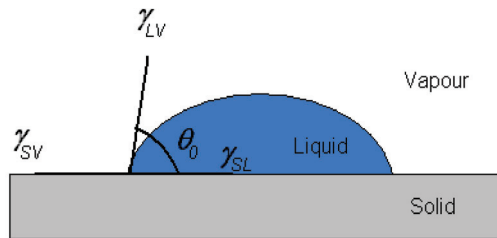


Figure 1. Schematic illustration of a water droplet on a flat solid surface. The contact angle (θ_0) is the angle between the solid-liquid interface (γ_{SL}) and the liquid-vapour interface (γ_{LV}). When the solid-vapour interface (γ_{SV}) increases, the γ_{SL} decreases but γ_{LV} and θ_0 increase, which is the case of a hydrophobic surface.

The Cassie-Baxter model [10] describes a state where the liquid does not follow the contours of the surface, but bridges across the cavities and sits upon a composite surface composed of both solid and air patches as shown in Figure 2c. Air remains trapped in cavities below the drop forming repellent ‘air pockets’. This results in strong hydrophobic surface properties. The Wenzel equation is modified by combining the contribution of the fractional area of wet surfaces and the fractional area with air pockets:

$$\cos \theta_{CB} = \varphi_{SL} \cos \theta_{SL} + \varphi_{LV} \cos \theta_{LV} \quad (4)$$

where θ_{SL} and θ_{LV} are the CA between solid-liquid and liquid-vapour respectively, φ_{SL} and φ_{LV} are the solid-liquid and liquid-vapour contact area per unit projected surface area, respectively:

$$\varphi_{SL} = \frac{A_{SL}}{A_F} \quad , \quad \varphi_{LV} = \frac{A_{LV}}{A_F} \quad (5), (6)$$

Since $\theta_{LV} = 180^\circ$, $\cos \theta_{LV}$ and the θ_{SL} becomes the CA for a planar surface (θ_0). Further, since, $\varphi_{SL} + \varphi_{LV} = 1$, equation (4) can be rewritten as:

$$\cos \theta_{CB} = \varphi_{SL} \cos \theta_0 + (1 - \varphi_{SL}) \cdot (-1) = \varphi_{SL} (\cos \theta_0 + 1) - 1 \quad (7)$$

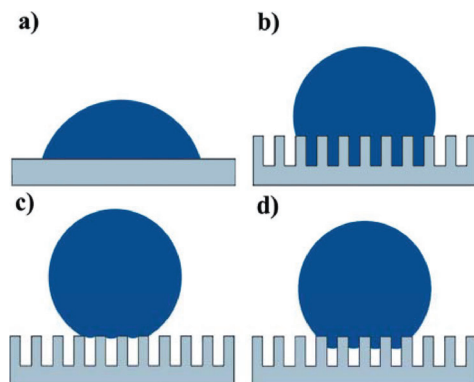


Figure 2. Schematic illustration of different regimes for wetting behaviour on rough surfaces; according to a) Young’s model (droplet on a flat surface), b) Wenzel’s model (homogeneous wetting of rough surface), c) Cassie-Baxter model (heterogeneous non-wetting of rough substrate), d) Intermediate state between the Wenzel and the Cassie models.

Several comparative studies of the wettability in the Wenzel and Cassie-Baxter regimes have been made [11, 12], showing that there is a critical value of φ_{SL} below which the Cassie-Baxter regime exists and above which the Wenzel regime is thermodynamically more stable and the transition means that the situation can be described as in Figure 2d. The transition between the two regimes occurs at a “critical” wetting angle (θ_c) defined by:

$$\cos \theta_c = \frac{\varphi_{SL} - 1}{R_f - \varphi_{SL}} \quad (8)$$

Thus, at CAs above the “critical” wetting angle air pockets should be present beneath the drop, according to the Cassie-Baxter model. The contact angle hysteresis (θ_H) is the difference in CA between the front and the back of a moving droplet along a solid surface. This can be written as

$$\theta_H = \theta_{adv} - \theta_{rec} \quad (9)$$

where θ_{adv} is the front angle of the droplet, called the advancing contact angle and θ_{rec} is the CA at the back of the droplet, called the receding contact angle. This phenomenon occurs due to the surface roughness and the heterogeneity of the sample. In the case of superhydrophobic surfaces with low water roll-off angle, the contact angle hysteresis is also low [13, 14]. A low water roll-off angle is vital for a superhydrophobic surface in order to receive a self-cleaning effect.

Two ways to examine the adhesion of the liquid to the substrate are to evaluate the roll-off angle (α) [15] or the driving force (F) [16] needed to get a liquid droplet rolling on the surface:

$$F = \frac{m \cdot g \cdot \sin \alpha}{w} = \varphi_{LV} (\cos \theta_{rec} - \cos \theta_{adv}) \quad (10)$$

where g is the force due to gravity, and m and w is the mass and width of the drop respectively. From equation (8), it can be found that a smaller difference between the advancing and receding CA will result in a lower roll-off angle. However, due to the small CA hysteresis in the case of superhydrophobic surfaces, the use of advancing and receding CA in this expression is discussed and may not be applicable [17]. Still it is used as a good starting point of discussion. Jung *et al.* [18] observed that for a homogeneous interface, increasing roughness leads to an increase in CA hysteresis (large difference $\theta_{adv} - \theta_{rec}$). However, for a heterogeneous air-water-solid interface an increase in roughness and φ_{LV} provides both high CA and small contact angle hysteresis.

There is a relationship between contact angle hysteresis and the surface roughness, however, no simple expression exists describing the hysteresis as a function of surface roughness.

The CA of a smooth hydrophilic surface increases with an increase of the liquid-vapour interface, φ_{LV} . When the roughness of the hydrophilic surface increases, the contact angle decreases, but a composite interface starts to form. At a certain high value of φ_{LV} the surface may become hydrophobic if it forms stable air pockets. This φ_{LV} -value may be a theoretical and unachievable value due to unstable properties of the air pockets but can be described as:

$$\varphi_{LV} \geq \frac{R_f \cos \theta_0}{R_f \cos \theta_0 + 1} \quad \text{for } \theta_0 < 90^\circ. \quad (11)$$

As mentioned above the air pockets in the Cassie-Baxter state make the drops roll off more easily because of smaller contact area and less adhesion forces between the droplet and the substrate. The surface shows low friction despite its roughness and a water droplet easily rolls off the surface [19, 20]. In the Wenzel state the liquid penetrates the pores and fills them entirely, which leads to a “sticky” surface behaviour of the rough surface [21]. The combination of a two-level roughness, with nanoscale roughness on the microscale roughness is believed to have great importance for and contribution to the ‘lotus effect’ [22]. However, superhydrophobic contact angles are also seen on e.g. rose petals and the ‘petal effect’ has been used [23] to describe a situation with high CA but also high adhesive force of the water droplet.

Applying a microscaled roughness is an effective way to increase the CA of a flat hydrophobic coating or substrate. The surface may become superhydrophobic, with an immediate low CA hysteresis and roll-off angle. However, when the water droplet stops and remains on the surface it sinks into the irregularities of the surface and forms a Wenzel state. This has been explained by the unstable composite liquid-vapour interface of a microscale roughness. In the Wenzel state the droplet gains a larger contact area to the roughened substrate than would be the case of a flat substrate. Thus, the adhesion force of the droplet increases and it sticks to the surface and will not roll off even when tilted to an angle of 90° .

Addition of ordered nanoscale pillars and pits to a flat hydrophobic substrate may trap air in the cavities of the surface, which enables a stabilised composite liquid-vapour interface [24]. A metastable Cassie-Baxter state is obtained. This is explained by the fact that the air is more stable in nanoscale cavities and pockets as the water molecules do not penetrate those pores as easily as microscale pores. The contact area decreases dramatically compared

to the case of a flat substrate, which in turn leads to a lower adhesion force between the droplet and the substrate. However, the surface is still very sensitive to water pressure, heterogeneities from the manufacturing process and mechanical wear and tear, because of the nanoscale roughness' incapability of lifting the water molecules at a larger distance from the surface.

In order to create a stable superhydrophobic surface with air-pockets between the solid and liquid, destabilizing factors such as capillary waves, nanodroplet condensation and liquid pressure should be avoided. This may be done by introduction of nanopattern on the microscale beads, which increases and pins the liquid-vapour interface and prevents nanodroplets from filling the cavities [25].

This two-level structure can be observed on lotus leaves, which contain microscale beads with hair-like nanoscaled structure on them. When water drops are placed on the leaves, strong water adhesion occurs if the leaf surfaces have lost their fuzzy nanoscale structures.

The dual scale roughness seems important for:

- amplifying the CA of the microscaled roughness
- creation of a stabilised composite interface: Cassie-Baxter state
- low CA hysteresis
- low sliding angle: the self-cleaning effect
- better resistance to damage and wear
- resistance to liquid pressure, capillary waves and nanodroplet condensation

High surface roughness with a combination of micro- and nanopatterns seems to be a requirement for stable, low roll-off angle superhydrophobic surfaces. However, self-cleaning surfaces require certain properties in order to be able to self-clean:

- Combination of morphology (structural roughness) and surface chemistry (hydrophobicity)
- High CA of about 150° or higher
- Low roll-off angle (about zero degrees)
- Low threshold sliding angle (CA hysteresis about zero degrees)
- Forms a stabilized liquid-vapour interface on the surface according to the Cassie-Baxter model
- Stable properties over a period of time

When a truly superhydrophobic surface is covered with water it looks all silvery due to a water-air interface on the surface, which reflects light. This can be used as an analytical method of the quality, stability and homogeneity of a superhydrophobic surface, as depicted in Figure 3 for a set of different

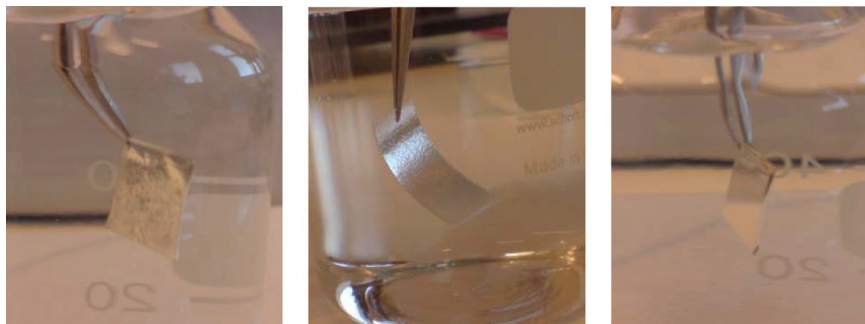


Figure 3. Close-ups from digital photo images of SH treated surfaces held by a tweezer under water. Left: SH mica, CA 159°; middle: SH PE-coated paperboard, CA 154°; right: SH silica substrate, CA 159°.

substrates, namely mica, PE coated paperboard and silica. The corresponding CAs were high in all three cases and it appears that macroscopic droplets of the size of 2 μl used for CA evaluation does not give any description of evenness of a SH coating.

Preparation methods of superhydrophobic surfaces

The preparation of superhydrophobic surfaces requires both preparation of a surface with a well-defined structure and roughness and hydrophobic surface chemistry. Therefore, in most cases the preparation involves two steps, but also the more desirable one-step methods have been developed.

The one-step methods require an initial hydrophobic chemistry of the substrate, the monomers or the coating, in order to get a superhydrophobic surface. These methods are divided in two sections, due to the approach of getting the surface roughness. The bottom-up approach builds up a surface roughness from molecules and monomers. The top-down approach forms the desired surface roughness of micro and nanoscale from macroscopic particles or the current substrate.

Bottom-up approach

Usually the development of a superhydrophobic surface includes toxic and environmental harmful fluorinated substances, in order to get low surface energy and good water repulsion. However, a water-borne superhydrophobic dispersion for paper board has been developed at YKI in Stockholm [4],

which consists of materials imparting both hydrophobic chemistry and the right surface structure. This one-step method is a good example of making environmental friendly superhydrophobic surfaces. iCVD is a one-step, solvent-free deposition technique. The conformal nature of the iCVD process enables nanoscale coating on complex substrates via radical polymerisation [26]. Electrospinning and electrohydrodynamics are methods of constructing thin fibres in nanoscale or microscale. A high voltage is applied between a nozzle, through which the sample solution is drawn, and a collector. The solvent evaporates and the solution jet solidifies and forms a rough film on the collector. The polymeric fluid must have conductivity in order to be electrospinnable and to form uniform fibres. Otherwise the surface tension tends to break the liquid jet into droplets, which is called Rayleigh instability. If this phenomenon dominates the process, beaded fibres or polymeric microdroplets will be formed instead of uniform fibres [26]. However, this state is favourable when preparing a superhydrophobic fabric [27]. During the electrospinning process a higher surface charge density on the solution-jet surface will result in smaller beads and thinner fibre diameters [28]. Producing porous materials that consist of a solid phase and a second phase that could be liquid or solid. The second phase is removed and a rough surface is obtained. This process has been simplified into a one-step method [29].

Top-down approach

Nanoporous anodic aluminium oxide has been used for pressure-driven imprint process.

The two most common template techniques are:

- *Template rolling press* [30] is a large area method which give well aligned polymeric nanopillar arrays with superhydrophobicity.
- *Template-based extrusion technique* [31] in which the polymer solution is extruded through the channels of the anodic aluminium oxide under pressure. This give arise to highly aligned polymer nanofiber films.

Even templates of polystyrene and silica spheres are commonly used [32, 33].

Plasma processing is commonly used and involves plasma polymerisation [34], plasma sputtering [35] and plasma etching [36, 37] in which a high-speed stream of monomer-plasma is shot in pulses at a substrate. The atoms of the shot element embed themselves at or just below the surface of the target. The physical, chemical and structural properties of the target are modified in the process. By using plasma polymerisation, plasma sputtering or plasma etching superhydrophobic surfaces can be obtained in one step.

Two-step methods

Even self-assembly of colloid particles on a solid substrate itself can serve as a rough surface structure [38, 39]. LbL and colloidal self-assembly are quite rich and advanced processes to fabricate thin film coatings. By varying the electrostatic interaction and hydrogen bonding, the molecular levels and film thicknesses are regulated. Usually, these methods are time-consuming and lead to a small-scale production of modified surfaces and morphology. The sol-gel processes have been used to fabricate superhydrophobic surfaces from a variety of materials [40, 41]. The sol-gel process is a process for making ceramic materials. The sol-gel process involves the transition of a system from a liquid (the colloidal “sol”) into a solid (the “gel”) phase. The sol-gel process allows the fabrication of materials with a large variety of properties [42]: ultra-fine powders, monolithic ceramics and glasses, ceramic fibres, inorganic membranes, thin film coatings and aerogels. Electrochemical Deposition (ECD) is a method to construct highly rough surface structures. A small electrical potential is used to create small nanoparticles on the substrate. High potential deposits larger nanostructures [43]. Even inorganic semiconductors and conducting polymer films can be fabricated by ECD [44]. By a combination of LbL and ECD a metal thread may be modified with polyelectrolyte multilayer through the LbL method. A metal may be electrodeposited onto the multilayer to form dendritic (hyperbranched) rough structures. Even a second level of roughness in nanoscale may be obtained by the ECD, if the LbL forms a micrometer surface structure in a first step [45]. Ion beam etching [46] is a technique using individual atoms in an ion beam to ablate the substrate. Reactive ion etching uses chemical reactivity of the ions to enhance the physical sputtering effect. It is possible to mask the substrate in order to protect those areas from being etched. Chemical etching [47, 48] is a process of using acids, bases or other chemicals to roughen the surface of a material. The chemicals, partly or completely, etch metals, semiconductor materials or glass and may remove unwanted materials from the substrate. KOH(aq) is commonly used for applications in printed circuit boards and for semiconductors. Some areas can be protected with non-reactive polymer mask or correspondent. Lithography includes photolithography, electron beam lithography, X-ray lithography, soft lithography, nanosphere lithography, which are techniques for creating large-area periodic patterns [49]. Nanosphere lithography is a technique for patterning periodic nanopore arrays over large areas [50]. A thin film of various materials may be applied onto a sacrificial template of spheres. The spheres are removed by calcination, which leaves the porous shells intact.

The required low energetic surface chemistry or hydrophobicity can be

received on hydrophilic substrates by using coatings, polymers, waxes or oxides of low-surface-energy materials such as The low surface energy is produced by using, coating, mixing or polymerising low-surface-energy materials such as alkylsilanes [51, 52], alkylthiols [32, 53], hydrophobic polymers [26, 54], hydrocarbon tails and waxes [18] or zinc oxide, ZnO [33, 55].

MATERIALS AND METHODS

Paperboard and cellulose probes

Cupforma Classic (StoraEnso, Sweden) both uncoated (230 g/m²) and PE-coated (205 g/m²) were used. Cellulose spheres from regenerated cellulose by the viscose process were obtained from Kanebo, Japan.

Silicon surfaces, cantilevers and silica spheres

Silicon wafers were supplied from WaferNet Inc, USA consisting of mono-crystalline sheets with double-polished sides having a naturally oxidized silica surface layer. The diameter is about 10 cm and the thickness 610 to 640 μm. Silica probes were borosilicate glass containing 75% silica and 25% oxides (boron oxide, sodium oxide, potassium oxide and calcium oxide) from Novascan, USA. AFM tipless cantilevers were ultrasharp silicon cantilevers from MikroMasch, USA (types CSC12/tipless/NoAl and NSC12/tipless/Cr-Au/50 while noncontact/tapping cantilevers used were silicon SPM cantilevers with tips from NanoWorld, Switzerland (type NCH-VS2-W). Borosilicate glass containing 75% silica and 25% oxides (boron oxide, sodium oxide, potassium oxide and calcium oxide) were provided from Novascan, USA.

Hydrophobic and SH formulations

Organic solvent hydrophobic solution contained 25.1 wt% Fluoropel 604A and 74.9 wt% HFE 7100. Organic solvent SH formulation contained 0.5 wt% Aerosil R972, 25.0 wt% Fluoropel 604A, 49.5 wt% HFE 7100 while the remaining weight fraction consists of acetone. Water borne SH coatings were prepared as described elsewhere [4].

The superhydrophobic coating contained methoxy-nonafluorobutane – a hydrofluoroether or HFE 7100 (3M, USA). HFE 7100 consists of two inseparable isomers with essentially identical properties with CAS# 163702-08-7 and 163702-07-6). A fluoropolymer was used, FluoroPel PFC 604A (Cytonix Corporation, USA) which contains 4 wt% of polyperfluorooctyl

methacrylate in HFE 7100 (No CAS#. available). Silica particles, Aerosil R972 (Degussa AG, Germany) were further used and consisted of hydrophobic fumed silica after treated with DDS (Dimethyldichlorosilane) based on a hydrophilic fumed silica with a specific surface area of 1100 m²/g and an average primary particle size of 16 nm, a carbon content of 0.6-1.2 wt% and a melting point of 1650 (\pm 75) °C (CAS#. 68611-44-9). For silanation a 1H,1H,2H,2H-Perfluorodecyltrichlorosilane, 96 % (Alfa Aesar, Germany) which is a three-functional fluorosilane with CAS# 78560-44-8. As wetting agent a sodium dodecyl sulphate (SDS) (Mallinckrodt Baker, Netherlands) with CAS# 151-21 was used at different concentration below, at and above the critical micelle concentration.

The water used in all experiments and sample preparations was prepared by means of a Milli-Q Plus Unit (Millipore, Bedford, MA, USA) including ion exchange, active carbon adsorption and reverse osmosis prior to the final 0.22 μ m filtration step. The water resistivity after this treatment was 18.2 M Ω -cm. The water was degassed prior to use by means of a water jet pump and a magnetic stirrer for 3 h until no bubble formation was observed at the magnet surface. To further improve the deaeration, the flask was sonicated in an ultrasonic bath for 30 minutes. NaCl pro analysis grade was obtained from Merck (Germany) and used as received. The silane used for the hydrophobizing silica particles and surfaces was tridecafluoro-1,1,2,2 tetra hydro-octyl trichlorosilane (ABCR, Germany). Colloidal silica particles with a radius, R, of 2.5 μ m (Bangs Laboratories, Inc. USA) were used as probes for the force measurements. A thermosetting resin (Epikote 1004, Resolution Europe B.V., The Netherlands) was employed to glue the colloidal probe to the cantilever.

Contact angles

Contact angle (CA) measurements were made using a portable goniometer (PGX, pocket model #50412) manufactured by Fibro Systems AB, Sweden. The volumes of the droplets used for the CA measurements were about 2 μ l. The attempts to measure the CA of superhydrophobic silicon surfaces experienced severe difficulties in order to get the droplet to remain on the surface. The superhydrophobic surfaces had a very low roll-off angle of close to zero degrees and usually the droplet was unable to stay on the small substrates prepared for the AFM colloidal probe measurements. Some superhydrophobic surfaces had small heterogeneities, which enabled CA measurements and CA measurements could usually be made after AFM measurements along the rim where the o-ring had dented the surface enough to increase the roll-off angle.

AFM colloidal probe

The colloidal probe measurements were made in a liquid cell by a Veeco – Multimode AFM with Nanoscope IIIa controller, with a Nanoscope Extender and a PicoForce™ from Digital Instruments, USA. The force data generated by Nanoscope software were evaluated by specially designed software. With this program normal force curves can be obtained. Multiple files can be loaded simultaneously and normalized force calculated by different calculations algorithms dependent on the type of torsional calibration.

Each measurement was repeated 80 to 180 times depending on how much the force curves varied. After 20 to 30 measurements at the same spot on the substrate, the probe was moved, the liquid cell rinsed and the probe approached the surface at a different spot. This was done in order to prevent the force measurement to be affected of local heterogeneities, impurities and local concentrations.

For the case of colloidal probe measurements at superhydrophobic substrates, macroscopic and microscopic bubbles were formed when MilliQ was added into the liquid cell. The macroscopic bubbles were removed from the liquid cell by using a relative high and pulsed water flow of a 10 ml syringe. The liquid pressure on the surface became quite high, in order to get rid of the bubbles and because of the small radius of the inlet tube. To avoid water escape from the liquid cell, the o-ring had to be tightly pressed to the substrate during addition of water. The 10 ml injector was left in the inset port to hinder the water from going backwards forming new macroscopic bubbles. When the surface of a superhydrophobic sample was covered by water the surface shifted in a spectrum of colours.

The colloidal probe measurements were made in the following media: MilliQ, deaerated MilliQ and in SDS solutions with 10%, 50% and 122% of CMC.

Some instrumental problems were experienced when trying to obtain force curves at single approach and at low approach to retract frequencies. The minimum frequency needed for getting continuous force curves was about 0.82 Hz and due to the long approach distance needed in the hydrophobic and superhydrophobic cases, the speed of the approach and retract became relatively high. This was good in order to minimize contingent capillary growth but gave rise to force curves in the form of loops. However, the attraction and jump-in was calculated according to the approach curve and the adhesion and adhesion distance was referred to the retraction curve.

Preparation of samples and WVTR evaluation

Samples were soaked in the solutions for 30 s. Solvent was evaporated in a fume hood for 15 min and then dried in oven for 10 min first at 50°C and then at 90°C for 10 min. Waterborne SH coatings were made using a laboratory rod coater. Samples were dried at 90°C for 2 min. Samples were stored in climate room (23°C and 55% RH). WVTR measurements were done according to Tappi Standard T448 om-97. Weight of anhydrous calcium chloride was 40 g. Data evaluation differed slightly from T448 om-97. Mass increase between 17 hours and 78 hours were fitted with linear regression to get the WVTR values.

Flexographic printing trials on SH coated paperboard

A paperboard coated with a water borne SH formulation was used. The flexographic ink used was a water-based acrylic obtained by mixing commercial cyan pigment dispersion (Flexiverse Blue 15:3) with the commercial vehicle Aquaten (Sun Chemical). The latter is a fully formulated vehicle comprising an alkaline blend of styrene-acrylate polymers, principally in the form of emulsions (dispersions), together with the full range of additives (e.g. cosolvents, waxes, wetting agents, defoamers) required for printing. The pigment dispersion and vehicle were mixed in the proportion 35:65 wt%. This ink is not tailored to printing on pigment coated board (but rather is more targeted to PE-coated board), but was chosen as its equilibrium surface tension is relatively high (around 35 mN/m), and thus its combination with the most SH substrate can be regarded as a worst case scenario.

This issue of wettability in relation to printing applications was checked prior to the laboratory printing trials by using dyne-liquids, commonly employed by industry for fast estimation of film surface energy, according to the test method described in ISO 8296 (former DIN 53364) and ASTM D2578. The liquid is applied as a broad line in a thin layer using, in this case, a felt pen (from Sherman Treaters, UK) and the surface energy is determined visually by judging how the liquid behaves on the surface within 2 s after application. If the test liquid shrinks and/or forms droplets, the substrate has lower surface energy than the test liquid, while if the liquid remains unchanged during these 2 s, the substrate is said to have surface energy at least equal to that of the liquid applied. The test liquids contain mixtures of formamide and ethylene glycol monoethyl ether and were available for every second unit in the range 30–56 mN/m.

The laboratory printing trials were made on a laboratory flexographic printing press IGT F1 (IGT Testing Systems, Netherlands). This press is

widely regarded as giving the best possible simulation of print quality obtained on a full industrial flexographic press.

The instrument hardware and settings were using a printing plate (fulltone) with plate cushion 2.6 mm (CyComp, DuPont, Germany), mounting foil 0.35 mm (CyComp, DuPont, Germany), mounting tape 0.1 mm (CT274, Scapa, UK), photopolymer 1.70 mm, hardness 57° Shore A (Nyloflex ART-D II, BASF, Germany), anilox volume: 8 ml/m² and cylinder force: 100, print cylinder-print substrate force: 100 N, printing speed 0.3 m/s, with three print cylinder rotations prior to printing.

Strips were cut from the central part of the board sheets to be of width approx. 5.5 cm, and length equal to the long axis of the sheet. A pair of these strips was mounted (top side up) by taping end-to-end on the printing sled,

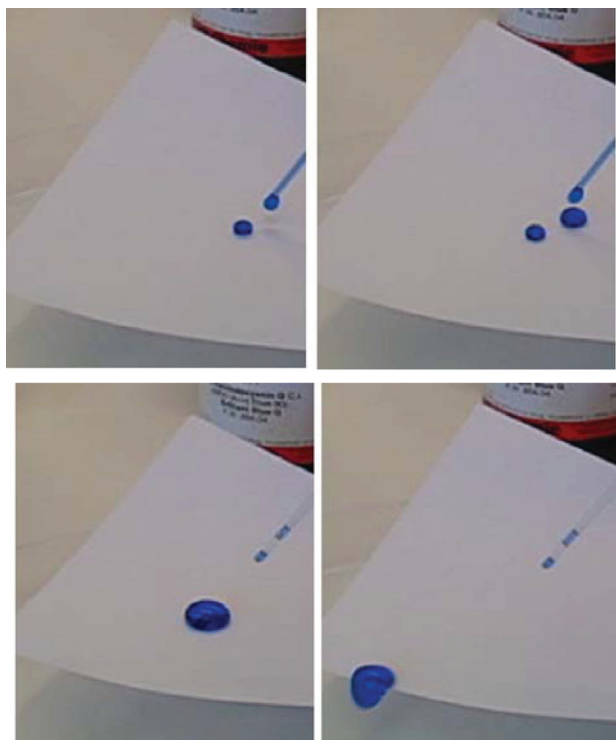


Figure 4. SH paper made by treatment of copy paper, illustrating water repellancy and self-cleaning through nanotechnology. Challenge is to meet demands on durability, adhesion, friction, food contact, in paper machine and packaging applications.

and printed simultaneously. The width of the printed stripe was 5 cm. Manual hot air drying was performed directly after printing, for a period of approx. 20 s.

RESULTS AND DISCUSSION

SH coatings on paper from organic solvents

Figure 4 displays a series of video image captures of blue-dyed water droplets on a dip-coated copy paper for an organic solvent based SH coating. The SH was achieved using this one-step treatment already at a coating weight of only about 1 g/m^2 but the disadvantage was organic solvent, fluoropolymers and expensive particulate formulations.

The solvent-based method was successfully used in testing new substrates and in development of fundamental understanding of the phenomena but was for the industrial applications abandoned due to obvious drawbacks of the used chemicals and treatments. Figure 5 shows another example using the same dip coating method and illustrates the mirror-like effect achieved by the air/vapour layer giving light reflectance.

CA measurements on these substrates are given in Figure 6 ranging from untreated paperboard to SH treated, both from an organic solvent and using a water borne SH treatment.

SH coatings were made on mica and these showed very high CAs. AFM

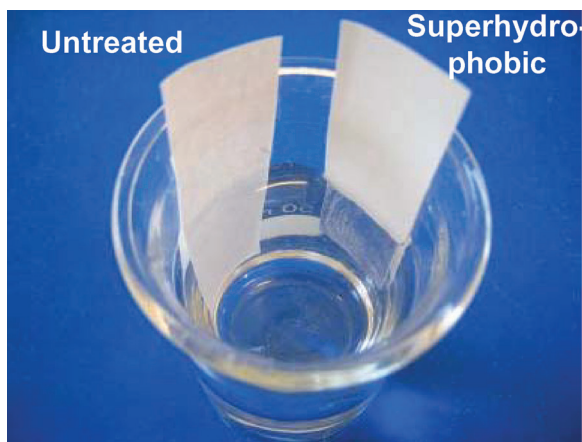


Figure 5. Air/vapour layer gives a mirror-like surface of the water-immersed SH treated paper.

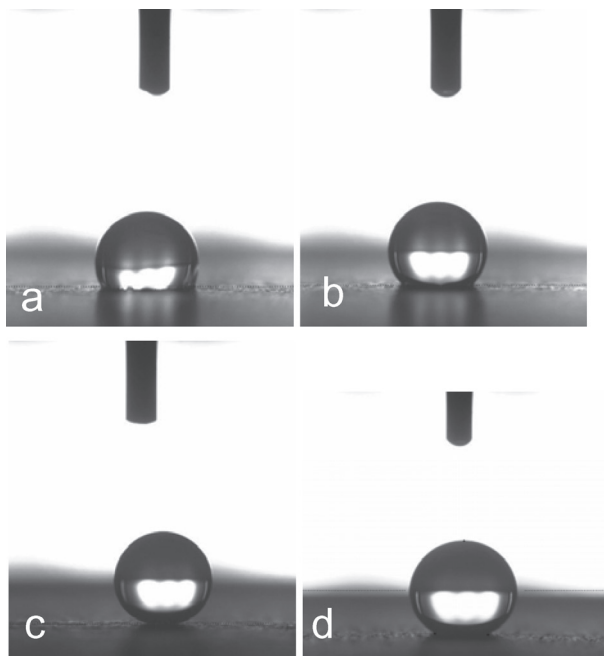


Figure 6. Contact angles for water droplets onto (a) untreated paperboard 117° , (b) hydrophobic 132° , (c) SH 154° and (d) water borne SH 145° , see below.

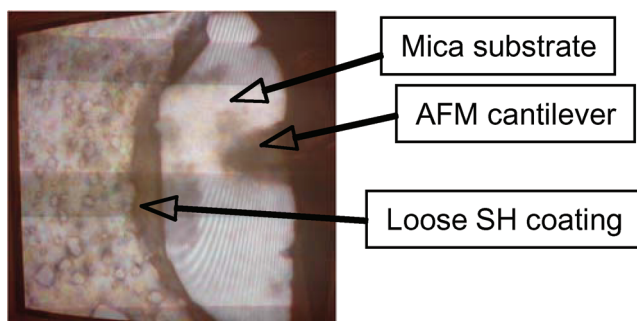


Figure 7. Photo of the AFM video capture during set-up of force measurements showing that the SH coating on mica was peeled off due to the water flushing of the liquid cell required to expel air pockets.

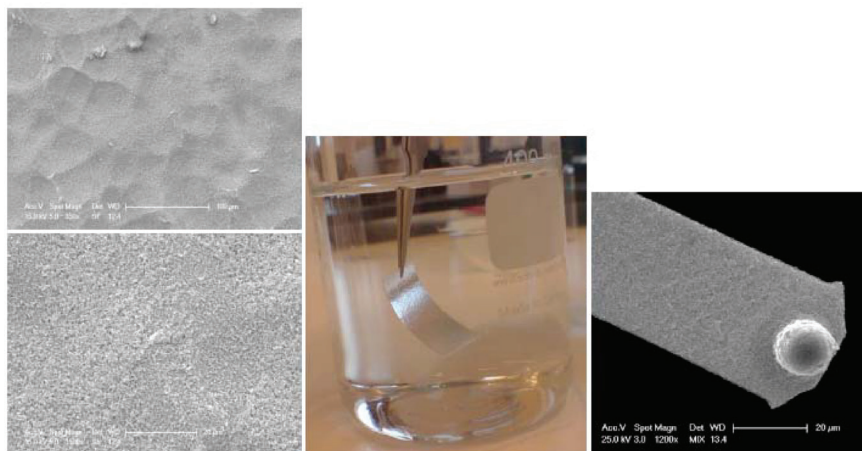


Figure 8. PE coated paperboard and cellulose probe sphere coated with organic solvent SH coating. Left: SEM of PE board (scale bar top 100 μm , bottom 20 μm), Surface roughness from AFM profilometry $10 \times 10 \mu\text{m}^2$ was 878 nm (peak-to-valley) and 142 nm (rms value). Middle: dip test in water showing a water repellent silvery surface of the SH treated sample. Right: SEM image of cellulose probe on AFM cantilever after SH treatment (scale bar 20 μm).

colloidal probe measurements were initiated but ceased because the coating was expelled from the mica surface as a result of the high water flushing during set-up of the experiments, Figure 7 shows the peeled-off SH coating captured from the AFM video image.

PE coated paperboard samples and cellulose probes were considered suitable candidates for SH treatment and measurements and PE coated board could quite easily be coated with organic solvent SH formulated and a cellulose probe could be mounted and treated in the same way, see Figure 8.

Force measurements were made in these system but interpretation of results proved difficult. The reason for this is unclear, however the experimental system SH-treated PE board in combination with silica probes (not cellulose probes) gave systematic results.

Interaction forces and influence of wetting agents on superhydrophobicity

Recent work by Singh *et al.* [56] shows that interaction forces between SH can be extremely long-range and that SH interaction can be viewed as an extension of the ‘hydrophobic’ force [57, 58]. Forces between surfaces in water

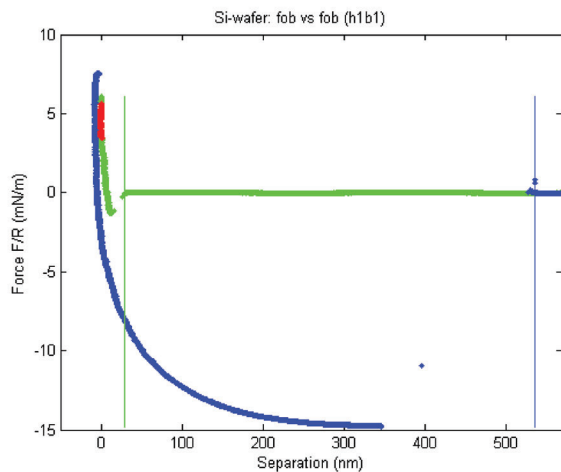
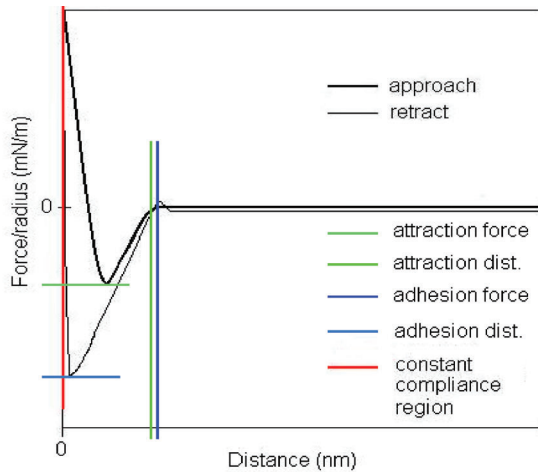


Figure 9. Top: Schematic of force-distance curve and definition of different parameters evaluated from the curves. Attraction distance is the jump-to-contact distance on approach of the two surfaces, etc. Bottom: Example of long-range hydrophobic attraction and adhesion between two hydrophobic surfaces in water.

mainly stem from van der Waals', electrostatic or steric interaction. These forces can extend from a few nanometers up to maybe 20 nm depending on conditions or even further for steric interactions between adsorbed polymer

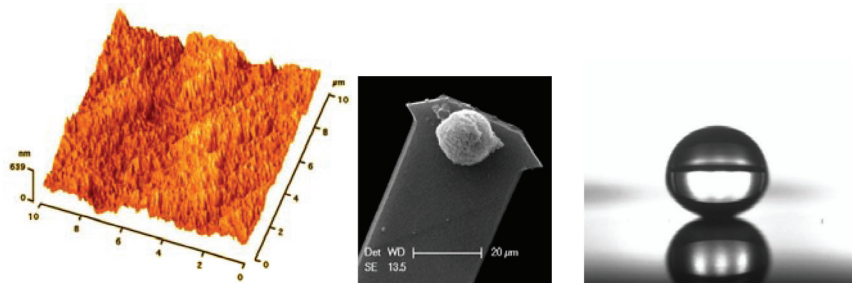


Figure 10. AFM, SEM images and water contact angle on silica substrates (surface and probe) used for interaction forces in SH systems.

layers. Since the first measurements of an even more long-range force [57] there has been debate about their origin as recently summarized by Wallqvist [59]. Recent work from our laboratory [60–62] reinforce the suggestion that the origin is from capillary forces from air/vapour cavities formed between two hydrophobic or superhydrophobic surfaces. The influence of wetting agents and surfactants on the contact angle for SH surfaces [2] suggest the importance of independent measures of wetting/dewetting behaviour.

Fundamental aspects of SH were investigated using silica wafers roughened by a particulate formulation containing methylated nanosize silica particles, fluoropolymer and fluorosurfactant, which were fixed to the substrate by calcinations, see Figure 10 [62, 63]. After hydrophobization by silylation, the forces between a colloidal superhydrophobized silica probe, made according to a similar procedure, and these surfaces by Atomic Force Colloidal Probe Microscopy were made suggest a long-range attraction distances up to 300 nm and a large influence of surfactant concentration.

Figure 11 shows force curves for the combination of a hydrophobic probe on a SH surface. Note the very long-range attraction and adhesion force extending to several micrometers.

The theories describing adhesion due to capillary condensation can be applied to other cases where surfaces are separated from each other in a non-wetting medium. One example is the case where two hydrophobic surfaces connected by an air/vapour cavity separate in water. A capillary meniscus between a sphere and a smooth flat surface causes an attractive force, which can be expressed as [64]:

$$\frac{F}{R} = 4\pi\gamma_{lv} \cos\theta \left[1 - \frac{D}{r_k} \right] \quad (12)$$

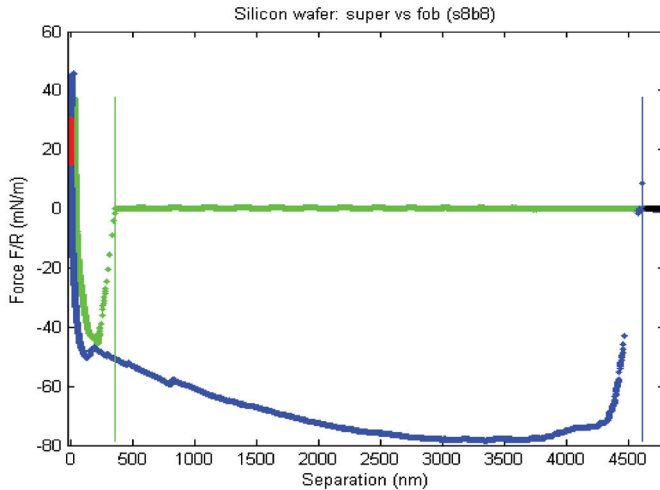


Figure 11. An example of a force curve made by a hydrophobic probe on a superhydrophobic substrate. Note the large attraction and adhesion distances.

where F is the attractive force, R the sphere radius, a a constant, γ_{lv} the interfacial energy between liquid and vapour, θ the contact angle of meniscus substance on surface substance, D the surface separation and r_K the Kelvin radius related to the size of the capillary condensate. It is shown [62] that the cavity model given in equation (12) fitted experimental data strongly suggesting that capillary forces determine that extent of long-range interaction between SH surfaces. Capillary condensates force as a function of RH, distance of separation and size of roughness features. Similar findings for silica and for cellulose systems in humid air have been reported [70, 71] in which a strong attraction occurs which increase as a function of e.g. RH.

A set of experiments were made for various combinations of hydrophilic, hydrophobic and superhydrophobic probes and surfaces, also with addition of surfactant and switching to deaerated water, see Figure 12. The very long-range interaction force is clear from these graphs, which summarize averages from more than twenty measurements for each combination. Addition of sodium dodecyl sulphate (SDS) surfactant decreases the attraction forces dramatically but these are restored to the same value for hydrophobic surfaces but not to the same level for SH surfaces. This may be an effect of remaining SDS adsorbed and stabilizing the air/vapour cavities.

A plausible explanation for the influence of surfactant on the dynamics of

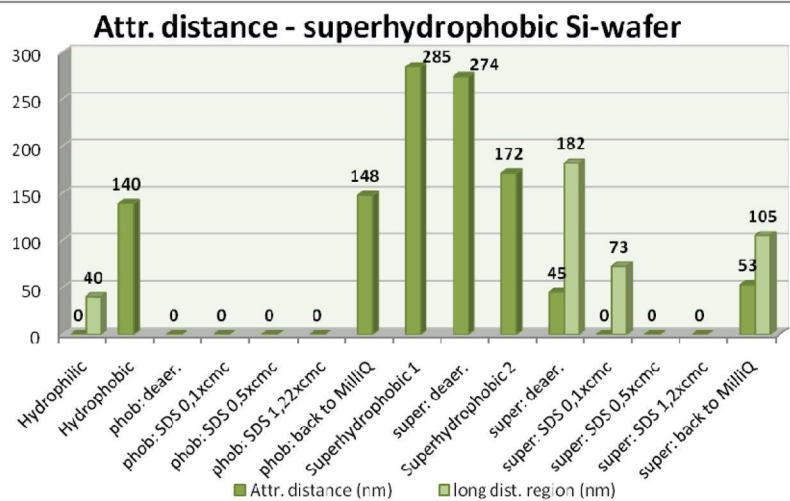
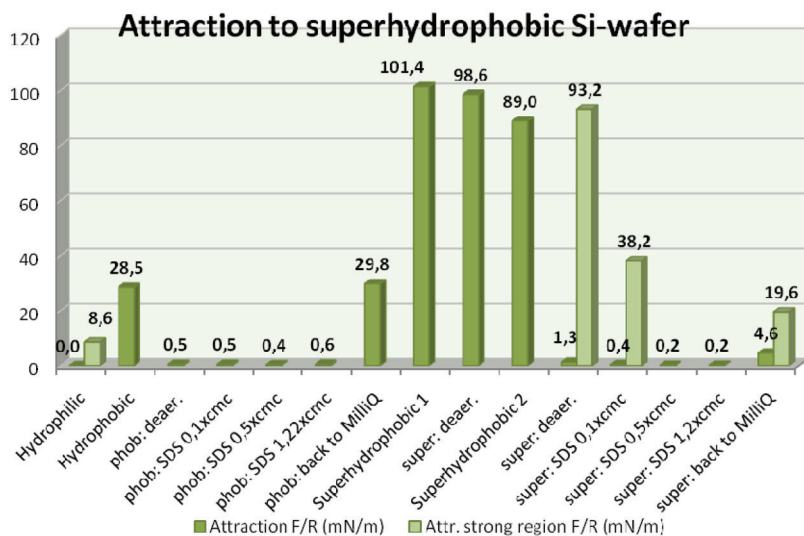


Figure 12. Attraction force (top) and distance (below) for different combinations of hydrophilic, hydrophobic and SH surfaces and probes. Different SDS concentrations were used for hydrophobic and SH combinations.

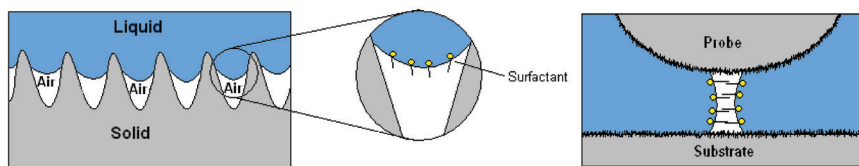


Figure 13. Left: Schematic illustration of surfactants remaining in the liquid-vapour interface of the rough SH surface. Some remaining surfactants would be difficult to completely remove, due to the stabilized interface. Right: Schematic illustration of an air-cappillary between SH probe sphere and SH surface stabilized by surfactants.

long-range interaction is given in Figure 13. SH coatings can thus be wetted and dewetted (i.e. restored in its superhydrophobicity) but the extent will depend on the concentration and type of surfactant. Wetting of SH surfaces has been examined to some detail before [2, 65, 66] but interaction forces have not been reported.

This type of behaviour will give rise to increased attraction and adhesion to the substrate.

WATER-BORNE SH COATINGS ON PAPER AND BOARD

A one-step water borne coating based on particles in a self-assembly with additives was developed. Figure 6 showed water contact angle on a paper-board surface for this type of coating.

The development of this coating was aimed at being used in industrial applications in a viable process and without introducing expensive or else unwanted material components. It was realized that depending on the type of application different measures for SH had to be used. The water contact angle (CA) is the most straightforward approach to defining SH, which should be over 150° . If self-cleaning aspects are developed the rolling angle is needed and is a good secondary indicator, especially of contact angle hysteresis. Long-term spreading is important in stain repellency and can be evaluated using a normalized stain size measure in which a dye solution droplet is carefully put on surface and to dry after which the spreading of the drop is normalized with respect to the initial liquid drop size. This reflects the penetration of liquid into the surface treatment, usually associated with a gradual decrease in CA. The hydrostatic resistance can be evaluated using a modified Cobb test and the mechanical stability of the surface by friction tests. Figure 14 shows that one measure is not enough and that different measures can give

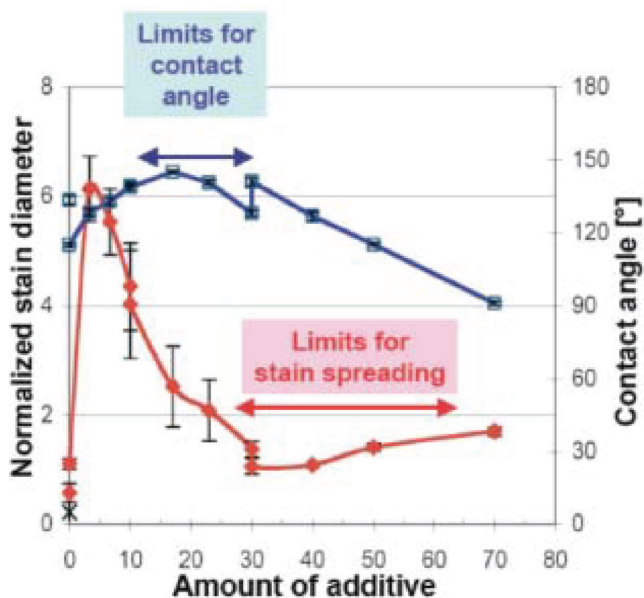


Figure 14. Two different measures of the degree of SH as a function of amount of additive in the water-borne SH coating on paper and board. The contact angle is at a maximum at 10 to 20 parts of additive whereas the stain diameter indicates a maximum degree of SH in the range of above 30 parts of additive.

significantly different results depending on, for example, additives needed in the water-borne coating.

Papermaking and packaging applications of superhydrophobicity

It is claimed that whereas SH give extreme water repellency, the water vapour transmission rate of these coatings would not be affected. This seems very logical considering the possibility for capillary condensation in a SH coating and based on the fact that hydrophobic coatings such as in papermaking is not a water vapour barrier. However, WVTR values for SH treatments or surfaces were not found in the literature so these were included in the present work. Table 1 give WVTR values for uncoated, hydrophobic and SH coatings on paperboard.

It is clear that WVTR is only very slightly affected by hydrophobic and SH treatments. Even with an extreme water repellency, there is water vapour transport across an air/vapour layer from a surrounding water layer as

Table 1. Water vapour transmission rates (WVTR) for untreated, hydrophobic and SH treated paperboard. Refer to Figure 6 for water contact angles for these coatings.

<i>Sample</i>	<i>Coat weight g/m²</i>	<i>WVTR g/(m² day)</i>	<i>Moisture content (w/w %)</i>
Untreated board	0	566	5.8
Hydrophobic	2.0*	554	
SH	3.7*	522	
Water borne SH	15	519	5.7

* Probably evenly distributed in the board.

function of the hydrostatic pressure and temperature or capillary condensation in the nano/micro-scale SH structure whereby water vapour is transported through a SH coating in contact with humid air. This is illustrated by the Kelvin equation, which in this case can be expressed as:

$$\ln RH = -\frac{2\gamma V_m}{r_K RT} \quad (13)$$

where *RH* is the relative humidity (%), γ liquid-air surface tension (N/m), V_m molar volume of water, r_K radius of water droplet or capillary (m), *R* the gas constant and *T* the absolute temperature (K). Already at 50 % RH there is capillary condensation in the nanoscale features present on a SH surface.

Possible concepts for extreme water repellency and water vapour barriers in packaging

It can be argued if SH coatings can at all be beneficial as barrier layers in packaging. Several possibilities however exist in combinations of vapour and gas barriers based on polymeric or wax coatings, which are given a boosted performance due to SH treatments. Renewable raw materials for barriers such as starches, bioplastics and proteins could reach specifications with smart combinations of SH treatment, either through coatings such as presented here or through e.g. electrospinning [67] combined with plasma functionalization or deposition as illustrated in Figure 15.

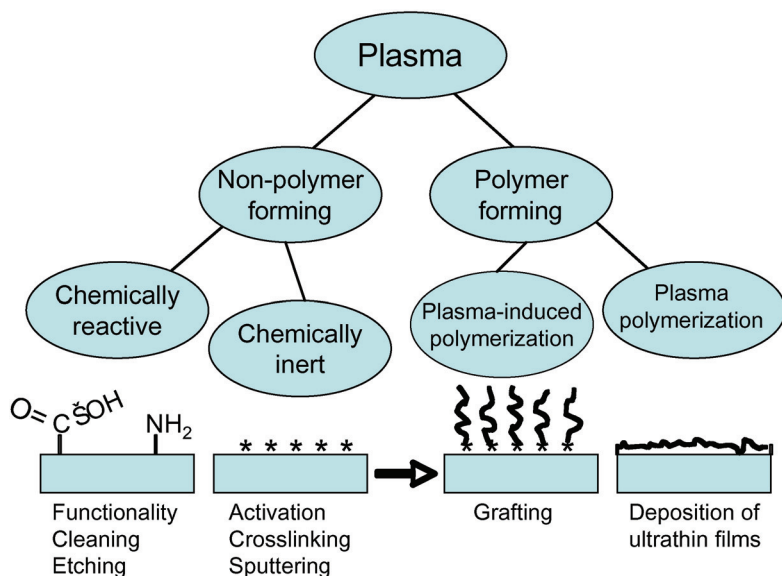


Figure 15. Plasma polymerisation or deposition can be used for functionalisation of surfaces (grafting of functional groups) and protective coatings (gas diffusion barriers). Recent advancements allow for these processes to be done using low-cost, high-speed treatments at atmospheric pressure.

Printing on SH treated paperboard

A key question regarding superhydrophobicity on packaging substrates is the effect of this treatment on their printability. For coated board flexography, offset and rotogravure are all used. Only flexography has been considered here, as the inks are typically water-based for this market, and so could be expected to be most affected by the SH. Offset printing also involves aqueous liquids, through the fountain solution, and also raises a number of issues. For rotogravure the solvent-based inks should in theory be less affected by the low surface energy of the substrate, however this printing technique is not a realistic consideration for the coated boards here, owing to their prohibitively high surface roughness induced by the large pigment used to create the texture required for SH.

Images of the dry lines (i.e. not after 2 s) on the SH coated board for four such pens (in steps of 6 mN/m) are displayed in Figure 16. The lowest of these four, namely 38 mN/m, did not display any dewetting retraction, suggesting that the printing ink (with surface tension even lower, i.e. 35 mN/m)

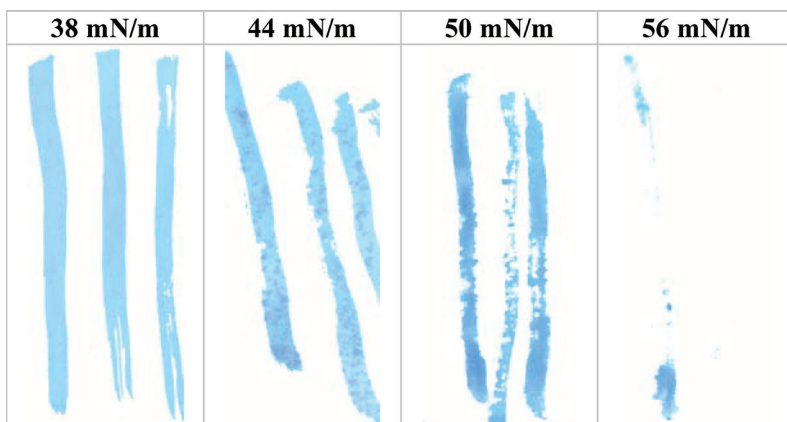


Figure 16. Scanned images of three lines for each of 4 dyne liquids applied with felt pen onto the SH coated board aimed for flexographic printing trials.

should be able to be transferred and maintain a relatively uniform distribution on the board surface. The next higher pen used (44 mN/m) only displayed slight edge contraction, suggesting that the effective surface energy of the substrate, by this measure, lies slightly above this value. Note however that the distribution of colorant is non-uniform within each stripe, with darker clusters due to local aggregation of the colorant. For the 50 mN/m pen edge contraction is significant (even after only 2 s), so the effective surface energy is judged as lying in the range 44–50 mN/m. Note that for the highest pen used (56 mN/m), only one, very broken, line is visible. For the other two sweeps of the pen no ink was transferred, i.e. the SH substrate completely refused to accept any ink.

The prints were not evaluated by any other means than visual inspection. From visual inspection all printed strips were uniform over their length and width, although did possess a slightly cracked/scratchy appearance. Figure 17 provides scanned images of the print. The texture of white branching channels derives from the anilox ruling, subsequently branching due to the Marangoni effect. This effect is commonly observed in flexography, and is not specific to the SH substrate here.

It can be concluded that such substrates are indeed printable with water-based flexography, with optimisation of ink and print settings (e.g. increasing the print cylinder-substrate nip load) able to further improve print quality. However, other post-printing issues such as print adhesion and abrasion

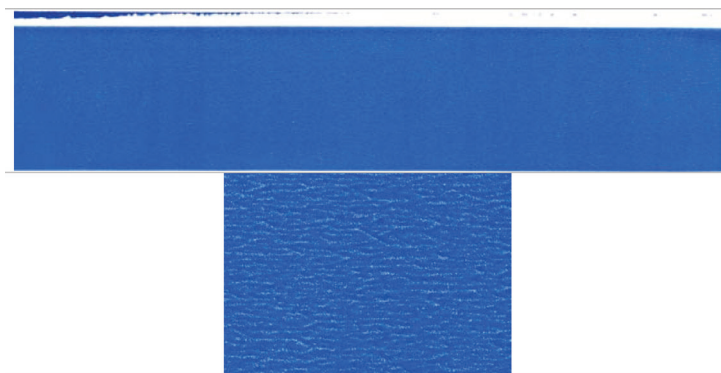


Figure 17. Scanned image of the printed strip (5 cm width) (top) and close-up of its fine texture (below).

resistance should also be considered. In this respect it is important to note that the printed substrate is no longer SH (checked by water drop spreading), even though the ink layer itself should have relatively low energy and some remnant of the spiky roughness texture from the underlying coat should still be present on the printed surface. This loss of SH is presumably due to the surfactants present in the ink. These results represent initial trials but show the possibility of using water-based printing methods on SH surfaces. The experimental fact that surfactants removes SH can be an obvious drawback but force measurements briefly presented here and in detail elsewhere [62], recent work [2] on different surfactant showing that some can be chosen not to alter the SH and the possibility of using thermolabile surfactants [68, 69] would suggest that SH can be remained or restored after a printing process. It would also suggest that printing techniques can be used to impart SH so that a printing ‘ink’ formulation contains the necessary surface roughness and hydrophobizing treatments in a one-step bottom-up approach.

CONCLUSIONS

Fundamental and applied aspects of superhydrophobicity related to paper-making and packaging has been reviewed and presented. Self-cleaning and water repellency using superhydrophobicity are among the most interesting potential applications. Very long-range interaction forces are measured between superhydrophobic surfaces. The range and value are decreased by addition of surfactant but can be restored. Combinations of superhydropho-

bic treatment with layers for improved gas and vapour barriers should be possible given a careful design of surface modification so that renewable raw materials performance can be augmented. Initial experiments of flexographic printing on superhydrophobic surfaces show how the surface is affected by surfactant and applied pressure.

ACKNOWLEDGEMENTS

The authors are grateful for contributions from past and present YKI colleagues: Robert Corkery, Andrew Fogden, Kenth Johansson, Isabel Mira, Mikael Sundin, Jouko Vyörykkä, and Viveca Wallqvist. Financial support through competence funding was received from Research Institutes of Sweden (RISE Holding AB, formerly IRECO Holding AB). The work is part of the R&D project Renewable Functional Barriers with financing from industry and VINNOVA, Swedish Agency for Innovation Systems through the Forestry Sector Research Programme.

REFERENCES

1. H.Y. Erbil, A.L. Demirel, Y. Avci and O. Mert. Transformation of a Simple Plastic into a Superhydrophobic Surface. *Science* 299(5611):1377–1380, 2003.
2. R. Mohammadi, J. Wassink and A. Amirfazli. Effect of Surfactants on Wetting of Super-Hydrophobic Surfaces. *Langmuir* 20(22):9657–9662, 2004.
3. C. Quan, O. Werner, L. Wagberg and C. Turner. Generation of Superhydrophobic Paper Surfaces by a Rapidly Expanding Supercritical Carbon Dioxide-Alkyl Ketene Dimer Solution. *Journal of Supercritical Fluids* 49(1):117–124, 2009.
4. A. Fogden, J. Vyoerykkae and R. Corkery. An Aqueous Dispersion, a Coated Subject and Use of an Aqueous Dispersion. Patent application WO 2008122617 (A1), YKI / Ytkemiska Institutet AB, 2008.
5. W. Barthlott and C. Neinhuis. Purity of the Sacred Lotus, or Escape from Contamination in Biological Surfaces. *Planta* 202(1):1–8, 1997.
6. X.J. Feng and L. Jiang. Design and Creation of Superwetting/Antiwetting Surfaces. *Advanced Materials* 18(23):3063–3078, 2006.
7. J. Genzer and K. Efimenko. Creating Long-Lived Superhydrophobic Polymer Surfaces through Mechanically Assembled Monolayers. *Science* 290(5499):2130–2133, 2000.
8. R.N. Wenzel. Resistance of Solid Surfaces to Wetting by Water. *Industrial and Engineering Chemistry* 28(8):988, 1936.
9. A. Torkkeli. Droplet Microfluidics on a Planar Surface, Doctoral dissertation, Department of Electrical Engineering, Helsinki University of Technology (VTT Publications 544), 2003.

10. A.B.D. Cassie and S. Baxter. Wettability of Porous Surfaces. *Transactions of the Faraday Society* 40:546, 1944.
11. J. Bico, U. Thiele and D. Quéré. Wetting of Textured Surfaces. *Colloids and Surfaces A: Physicochemical and Engineering Aspects* 206(1–3):41, 2002.
12. M. Callies and D. Quere. On Water Repellency. *Soft Matter* 1(1):55–61, 2005.
13. C.W. Extrand. *Langmuir* 18:7991–7999, 2002.
14. J. Kijlstra, K. Reihs and A. Klami. *Colloids Surfaces A* 206:521–529, 2002.
15. C.G.L. Furmidge. *Journal of Colloid and Interface Science* 17:309, 1962.
16. E. Wolfgram and R. Faust., Academic Press, London, 1978.
17. B. Krasovitski and A. Marmur. *Langmuir* 21:3881–3885, 2005.
18. Y.C. Jung and B. Bhushan. Contact Angle, Adhesion and Friction Properties of Micro- and Nanopatterned Polymers for Superhydrophobicity. *Nanotechnology* 17:4970–4980, 2007.
19. D. Quéré, A. Lafuma and J. Bico. Slippery and Sticky Microtextured Solids. *Nanotechnology* 14:1109, 2003.
20. A. Otten and S. Herminghaus. *Langmuir* 20:2405, 2004.
21. N.A. Patankar. *Langmuir* 20:8209, 2004.
22. Y.T. Cheng and D.E. Rodak. *Nanotechnology* 17:1359–1362, 2006.
23. L. Feng, Y.A. Zhang, J.M. Xi, Y. Zhu, N. Wang, F. Xia and L. Jiang. Petal Effect: A Superhydrophobic State with High Adhesive Force. *Langmuir* 24(8):4114–4119, 2008.
24. E. Martinez, K. Seunarine, H. Morgan, N. Gadegaard, C.D.W. Wilkinson and M.O. Riehle. Superhydrophobicity and Superhydrophilicity of Regular Nanopatterns. *Nanoletters* 10:2097–2103, 2005.
25. B. Bhushan and Y.C. Jung. Wetting Study of Patterned Surfaces for Superhydrophobicity. *Ultramicroscopy* 107:1033–1041, 2007.
26. M. Ma, Y. Mao, M. Gupta, K.K. Gleason and G.C. Rutledge. Superhydrophobic Fabrics Produced by Electrospinning and Chemical Vapor Deposition. *Macromolecules* 38:9742–9748, 2005.
27. L. Jiang, Y. Zhao and J. Zhai. *Angewandte Makromolekulare Chemie* 43:4338, 2004.
28. Z.M. Huang, Y.Z. Zhang, M. Kotaki and S. Ramakrishna. *Composites Science and Technology* 63:2223, 2003.
29. Q.D. Xie, G.Q. Fan, N. Zhao, X.L. Guo and J. Xu. *Advanced Materials* 16:1830, 2004.
30. C.W. Guo, L. Feng, J. Zhai, G.J. Wang, Y.L. Song, L. Jiang and D.B. Zhu. Large-Area Fabrication of a Nanostructure-Induced Hydrophobic Surface from a Hydrophilic Polymer. *Chemical Physics Communications* 5:750–753, 2004.
31. L. Feng, S.H. Li, H.J. Li, J. Zhai, Y.L. Song, L. Jiang and D.B. Zhu. *Angewandte Makromolekulare Chemie* 41:1221, 2002.
32. M.E. Abdelsalam, P.N. Bartlett, T. Kelf and J. Baumberg. *Langmuir* 21:1753, 2005.
33. Y. Li, W. Cai and G. Duan. *Journal of Colloid and Interface Science* 287:634–639, 2005.

34. W. Chen, A.Y. Fadeev, M.C. Hsieh, D. Öner, J. Youngblood and T.J. Mccarthy. *Langmuir* 15:3395, 1999.
35. J.P. Youngblood and T.J. Mccarthy. *Macromolecules* 32:6800, 1999.
36. A. Kojima, Y. Izumi, Y. Kowase, T. Ohte and K. Miyashita. *Journal Photopolymer Science and Technology* 11:321, 1998.
37. M. Lejeune, L.M. Lacroix, F. Brétagnol, A. Valsesia, P. Colpo and F. Rossi. *Plasma-Based Processes for Surface Wettability Modification. Langmuir* 22:3057–3061, 2006.
38. J.Y. Shiu, C.W. Kuo, P. Chen and C.Y. Mou. *Chemical Materials* 16:561, 2004.
39. J.L. Zhang, L.J. Xue and Y.C. Han. *Langmuir* 21:5, 2005.
40. X.J. Feng, L. Feng, M.H. Jin, J. Zhai, L. Jiang and D.B. Zhu. *J Am Chem Soc* 126:62–63, 2004.
41. N.J. Shirtcliffe, G. Mchale, M.I. Newton, C.C. Perry and P. Roach. *Chem. Commun.:*3135–3137, 2005.
42. M. Miwa, A. Nakajima, A. Fujishima, K. Hashimoto and T. Watanabe. *Langmuir* 16:5754, 2000.
43. H. Yan, K. Kurogi, H. Mayama and K. Tsujii. *Angewandte Makromolekulare Chemie* 44:3453, 2005.
44. X.T. Zhang, O. Sato and A. Fujishima. *Langmuir* 20:6065, 2004.
45. N.J. Shirtcliffe, G. Mchale, M.I. Newton, G. Chabrol and C.C. Perry. *Advanced Materials* 16:1929, 2004.
46. X.Y. Song, J. Zhai, Y.L. Wang and L. Jiang. *J. Phys. Chem.* 109:4048–4052, 2005.
47. H. Schröder and E. Obermeier. *Journal of Microelectromechanical Systems* 10:1, 2001.
48. K. Sato. *Sensors and Actuators A* 64:87–93, 1988.
49. M. Callies, Y. Chen, F. Marty, A. Pepin and D. Quéré. *Microelectron. Eng.* 78:100–105, 2005.
50. R. Furstner, W. Barthlott, C. Neinhuis and P. Walzel. *Langmuir* 21:956–961, 2005.
51. B.T. Qian and Z.Q. Shen. *Langmuir* 21:9007–9009, 2005.
52. H.M. Shang, Y. Wang, S.J. Limmer, T.P. Chou, K. Takahashi and G.Z. Cao. *Thin Solid Films* 472:37–43, 2005.
53. X. Zhang, F. Shi, X. Yu, H. Liu and Y. Fu. *J. Am. Chem. Soc.* 126:3064–3065, 2004.
54. W. Ming, D. Wu, R. Van Benthem and G. De With. *Nano Lett.* 5:2298–2301, 2005.
55. L. Huang, S.P. Lau, H.Y. Yang, E.S. Leong, S.F. Yu and S. Praver. *J. Phys. Chem.* 109:7746–7748, 2005.
56. S. Singh, J. Houston, F. Van Swol and C.J. Brinker. *Superhydrophobicity: Drying Transition of Confined Water. Nature* 442(7102):526, 2006.
57. J. Israelachvili and R. Pashley. *The Hydrophobic Interaction Is Long-Range, Decaying Exponentially with Distance. Nature* 300(5890):341–342, 1982.
58. J.N. Israelachvili and R.M. Pashley. *Measurement of the Hydrophobic Interaction between 2 Hydrophobic Surfaces in Aqueous-Electrolyte Solutions. Journal Of Colloid And Interface Science* 98(2):500–514, 1984.
59. V. Wallqvist. *Interactions between Non-Polar Surfaces in Water: Focus on Talc,*

- Pitch and Surface Roughness Effects, Doctoral dissertation, Chemical Science and Engineering, Surface and Corrosion Science, KTH, Royal Institute of Technology, Stockholm, Sweden, 2009.
60. V. Wallqvist, P.M. Claesson, A. Swerin, C. Östlund, J. Schoelkopf and P. Gane. Adhesive and Long-Range Capillary Forces between Hydrophobic Surfaces in Water: Effect of Surface Topography. In XIVth Fundamental Research Symposium, "Advances in Pulp and Paper Research" (In Press), (ed. FRC), Oxford, UK.
 61. V. Wallqvist, P.M. Claesson, A. Swerin, P. Gane and J. Schoelkopf. Influence of Surface Topography on Adhesive and Long-Range Attractive Forces between Hydrophobic Surfaces in Water. *Langmuir* (submitted)
 62. A. Swerin and M. Wåhlander. Interaction Forces between Superhydrophobic Surfaces Using AFM Colloidal Probe Measurements in Liquid Cell. *Langmuir* (Under submission), 2009.
 63. M. Wåhlander. Development and Characterization of Superhydrophobic Surfaces – AFM Colloidal Probe Measurements between Superhydrophobic, Hydrophobic and Hydrophilic Surfaces in Liquid Cell, Master of Science Thesis, Department of Fiber and Polymer Technology, KTH, School of Chemical Science and Engineering, Stockholm, 2008.
 64. J.N. Israelachvili. *Intermolecular and Surface Forces*. 2nd Ed., Academic Press, Inc., London 1992.
 65. F.M. Chang, Y.J. Sheng, H. Chen and H.K. Tsao. From Superhydrophobic to Superhydrophilic Surfaces Tuned by Surfactant Solutions. *Applied Physics Letters* 91(9) 2007.
 66. M. Ferrari, F. Ravera, S. Rao and L. Liggieri. Surfactant Adsorption at Superhydrophobic Surfaces. *Applied Physics Letters* 89(5) 2006.
 67. M.L. Ma and R.M. Hill. Superhydrophobic Surfaces. *Current Opinion In Colloid & Interface Science* 11(4):193–202, 2006.
 68. M. Andersson. Printing Inks with Enhanced Water Resistance and Adhesion Properties – Inks with Increased Resistance Towards Water and Water-Borne Chemicals and Enhanced Adhesion Towards Secondary Coatings. YKI Unpublished.
 69. M. Andersson. Surfactant Precursor. Patent application WO2007/ 051632 A2, YKI, 2007.
 70. A.A. Feiler, P. Jenkins and M.W. Rutland. Effect of Relative Humidity on Adhesion and Frictional Properties of Micro- and Nano-Scopic Contacts. *Journal Of Adhesion Science And Technology* 19(3–5):165–179, 2005.
 71. A.A. Feiler, J. Stiernstedt, K. Theander, P. Jenkins and M.W. Rutland. Effect of Capillary Condensation on Friction Force and Adhesion. *Langmuir* 23(2):517–522, 2007.

Transcription of Discussion

ON FUNDAMENTALS AND APPLICATIONS OF SUPERHYDROPHOBICITY IN PAPERMAKING AND PACKAGING

Agne Swerin and Martin Wåhlander

YKI, Institute for Surface Chemistry, Box 5607, SE-114 86 Stockholm,
Sweden

Mark Kortschot University of Toronto

The superhydrophobicity comes from the bumpy pattern, but can you tell us anything about the limit on the lateral size of those bumps? In other words, how big can that texture be and still produce superhydrophobicity?

Agne Swerin

When it comes to these Cassie-Baxter and Wenzel type of regimes, you can look in the reviews to get the feeling for the geometries that you need. The height of the pillars schematically should be something like 5 or maybe 10 times larger than the distance between the pillars. You need to achieve that both at the nanometer scale and at the micrometer scale, but they cannot be larger, as you have to have the right roughness to combine with hydrophobicity to achieve superhydrophobicity.

Mark Kortschot

Okay. Thank you.

Lars Wågberg KTH

Thank you, Agne, for a really nice presentation that raises a lot of new ideas

Discussion

in my brain at least. In one of your first slides you mentioned that it was possible to create superhydrophobicity, or hydrophobicity, from inherently hydrophilic material; what exactly do you mean by that?

Agne Swerin

If you combine surface roughness with hydrophobicity, then you can achieve superhydrophobicity. If you start with an hydrophilic material and create the right type of surface roughness, which would give very small contact area with a liquid, then you can achieve a high water contact angle – not superhydrophobicity, but hydrophobicity.

Lars Wågberg

But what do you mean by high apparent contact angle in that case, and what would be the intrinsic contact angle for that material?

Agne Swerin

Well the apparent contact angle would be high but could decrease quite rapidly as a function of time because of local wetting.

Lars Wågberg

The reason why I am asking is that, in our modeling that you kindly mentioned here, we found that you can actually create a hydrophobic surface for contact angles slightly lower than 90 degrees, but not much. Maybe that is what you mean also?

Agne Swerin

Thanks.

Wolfgang Bauer Graz University of Technology

Did you look at the aspect of recycling superhydrophobic materials in paper making?

Agne Swerin

Yes, that is an important part of paper making, of course, and we did not

look into that But when you re-cycle, for example, by washing or flotation, you are adding surface-active compounds which could lead to wetting of a superhydrophobic surface, so I think it would possible to get the material back into the process.